Title: Inhibition of the shade avoidance response by formation of non-DNA binding bHLH heterodimers.

Authors: Hornitschek P, Lorrain S, Zoete V, Michielin O, Fankhauser C

Journal: The EMBO journal

Year: 2009 Dec 16

Volume: 28

Issue: 24

Pages: 3893-902

DOI: 10.1038/emboj.2009.306

Title page

Inhibition of the shade avoidance response by formation of non-DNA binding bHLH heterodimers.

Patricia Hornitschek [1], Séverine Lorrain [1], Vincent Zoete [2], Olivier Michielin [2] and Christian Fankhauser [1, 3]

[1] Center for Integrative Genomics, University of Lausanne, Genopode Building, CH-1015 Lausanne, Switzerland.

[2] Swiss Institute of Bioinformatics, Molecular Modeling Group, Genopode Building CH-1015 Lausanne, Switzerland

[3] Corresponding author:
Christian Fankhauser
christian.fankhauser@unil.ch
phone: ++41 21 692 3941
FAX: ++41 21 692 3925

Character count: 47377

Running title: HFR1 inhibits PIF DNA binding

Key words: Shade avoidance/phytochrome/HFR1/PIF/bHLH factor

Subject category: Plant Biology

Abstract

In shade-intolerant plants such as Arabidopsis a reduction in the red/far-red (R/FR) ratio, indicative of competition from other plants, triggers a suite of responses known as the shade avoidance syndrome (SAS). The phytochrome photoreceptors measure the R/FR ratio and control the SAS. The Phytochrome Interacting Factors 4 & 5 (PIF4 and PIF5) are stabilized in the shade and required for a full SAS while the related bHLH factor HFR1 (long Hypocotyl in FR light) is transcriptionally induced by shade and inhibits this response. Here we show that HFR1 interacts with PIF4 and PIF5 and limits their capacity to induce the expression of shade marker genes and to promote elongation growth. HFR1 directly inhibits these PIFs by forming non-DNA binding heterodimers with PIF4 and PIF5. Our data indicate that PIF4 and PIF5 promote the SAS by directly binding to G-boxes present in the promoter of shade marker genes, but their action is limited later in the shade when HFR1 accumulates and forms non-DNA binding heterodimers. This negative feed-back loop is important to limit the response of plants to shade.

Introduction

Light is a source of energy for plants, but also an important source of information about the surrounding environment. Since plants are sessile photosynthetic organisms it is of major importance that they adapt their growth habit to changing light conditions. One well-studied phenomenon is the shade avoidance response. In high vegetative density the red/far-red (R/FR) ratio decreases because red light is absorbed by photoactive pigments of neighbor plants, whereas FR light is mainly transmitted and reflected (Ballare, 1999; Franklin, 2008; Vandenbussche et al., 2005). This change of light quality is detected by the phytochrome family of R/FR photoreceptors (phyA-phyE in Arabidopsis) and leads to the shade avoidance syndrome (SAS) (Franklin and Whitelam, 2005). In order to reach direct sunlight several morphological changes take place. The SAS includes elongation growth of stems and petioles at the expense of development of leaf blades and storage organs. In addition plants have elevated leaf angles (hyponasty), increased apical dominance leading to reduced lateral branching and flowering is accelerated (Ballare, 1999; Franklin and Whitelam, 2005; Vandenbussche et al., 2005). Although the SAS can negatively impact biomass production and seed yield it is of major adaptive significance in natural environments (Franklin and Whitelam, 2005; Izaguirre et al., 2006; Moreno et al., 2009). Moreover, the study of SAS is of direct relevance for agriculture where high-density planting is common practice.

By monitoring changes in the R/FR ratio the phytochrome photoreceptors are the primary regulators of the SAS (Franklin and Whitelam, 2005). In Arabidopsis phyB plays a predominant function although phyD and phyE also contribute to this adaptive response (Devlin et al., 1998; Devlin et al., 1999). A drop in the R/FR ratio leads to rapid changes in the level of numerous transcripts including several encoding transcription factors (Carabelli et al., 1996; Devlin et al., 2003; Salter et al., 2003; Sessa et al., 2005; Sorin et al., 2009) . Moreover, numerous genes coding for hormone signaling components or metabolic enzymes are rapidly induced by shade (Devlin et al., 2003). Several hormones including auxin, GA, brassinosteroids and ethylene have been functionally linked to shade-regulated growth processes (Alabadi and Blazquez, 2009; Hisamatsu et al., 2005; Kurepin et al., 2007a; Kurepin et al., 2007b; Morelli and Ruberti, 2002; Vandenbussche et al., 2005; Carabelli et al., 2007; Tanaka et al.,

2002). The hormone-light connection has most extensively been studied for auxin (Morelli and Ruberti, 2002; Roig-Villanova et al., 2007; Carabelli et al., 2007; Tanaka et al., 2002). Both auxin transport and biosynthesis have been shown to be required for an effective SAS (Kanyuka et al., 2003; Morelli and Ruberti, 2002; Tao et al., 2008; Carabelli et al., 2007; Tanaka et al., 2002). In particular a reduction of the R/FR ratio leads to a rapid increase of auxin biosynthesis. This upregulation critically depends on the TAA1 aminotransferase, which catalyzes the first step in a newly described auxin biosynthetic pathway (Stepanova et al., 2008; Tao et al., 2008). While numerous aspects of the SAS strictly depend on TAA1 several early shade marker genes are still normally upregulated in the *sav3/taa1* mutant (Tao et al., 2008).

PIF4 and PIF5 (Phytochrome Interacting Factors 4&5) represent a direct link between the phytochromes and the regulation of shade marker genes (Lorrain et al., 2008). In high R/FR PIF4 and PIF5 are degraded presumably upon interaction with the Pfr conformer of the photoreceptor (Nozue et al., 2007; de Lucas et al., 2008; Lorrain et al., 2008; Shen et al., 2007). Upon transfer into the shade the phytochrome photo-equilibrium shifts towards Pr, which has reduced affinity for the PIFs and thus stabilizes those proteins leading to the expression of shade-induced genes (Lorrain et al., 2008). Interestingly several early shade marker genes are inhibitors of SAS, showing that this system includes a negative feedback loop which prevents an excessive response (Roig-Villanova et al., 2007; Sessa et al., 2005). For example, PAR1 and PAR2 (Phytochrome rApidly Regulated 1 and 2) coding for small bHLH proteins are involved in the down-regulation of genes involved in auxin responses (Roig-Villanova et al., 2007). HFR1, which codes for a bHLH protein related to PIF4 and PIF5 also plays an important role to prevent an excessive response to shade (Sessa et al., 2005). Although HFR1 belongs to the bHLH family several sequence features distinguish its basic domain. This lead to the proposal that HFR1 either does not bind to the canonical E-box or does not bind to DNA at all. However its molecular mode of action remains unknown (Fairchild et al., 2000).

In this study we examined the mode of HFR1 action focusing on responses to shade. Using a combination of genetic and biochemical experiments we show that HFR1 prevents an exaggerated shade avoidance response by forming non-DNA binding heterodimers with PIF4 and PIF5.

Results

Genetic relationship between *PIF4*, *PIF5* and *HFR1* during shade avoidance.

The bHLH transcription factors, PIF4 and PIF5, are necessary for a complete shade avoidance response, whereas the related bHLH protein HFR1 is involved in a negative mechanism, which prevents an excessive shade avoidance response (Lorrain et al., 2008; Sessa et al., 2005). In order to gain mechanistic insight into the regulatory network of those bHLH class transcription factors we first studied the genetic interaction between mutants defective for those proteins. We generated all possible mutant combinations between *hfr1*, *pif4* and *pif5* and studied their growth under high and low R/FR (to simulate shade) keeping Photosynthetically Active Radiation (PAR) constant. We concentrated our analysis on *hfr1*, *pif4pif5* and the *hfr1pif4pif5* triple mutant, because *pif4pif5* has a more severe phenotype than each single mutant (Lorrain et al., 2008). *hfr1pif4* and *hfr1pif5* double mutants essentially showed intermediate phenotypes between the two parental lines (data not shown). All tested genotypes were grown for 4 days in high R/FR then either kept in the same conditions or transferred into low R/FR for additional 4.5 days. The wild type, *hfr1*, *pif4pif5* and *hfr1pif4pif5* responded to low R/FR with elongation of the hypocotyls (Figure 1A). As previously reported the *pif* mutants had the opposite phenotype of *hfr1* in low R/FR shade-mimicking conditions; *pif4pif5* had a shorter hypocotyl and *hfr1* displayed an elongated hypocotyl compared to the wild type. Analysis of the triple mutant showed that the *pif4pif5* was largely epistatic over the *hfr1* mutant phenotype. This experiment confirmed that a reduction in the R/FR ratio still induced elongation of the hypocotyl in *pif4pif5*, indicating that in addition to PIF4 and PIF5 other pathways promote the SAS (Figure 1) (Lorrain et al., 2008). The recently discovered TAA1 aminotransferase and members of the homeodomain-leucine zipper class II transcription factors are good candidates for this (see discussion) (Sorin et al., 2009; Tao et al., 2008).

Changes in the R/FR ratio have profound effects on gene expression (Devlin et al., 2003; Sessa et al., 2005; Salter et al., 2003) . We analyzed the expression of the early shade marker genes *PIL1* coding for a PIF-related transcription factor (Salter et al., 2003) and *XTR7*, coding for a xyloglucan endotransglycosylase-related protein, by quantitative-PCR (Q-PCR). We chose *XTR7* because its levels respond rapidly to

shade and because it encodes a protein that is presumably directly related to the cell elongation process (Devlin et al., 2003; Salter et al., 2003). Moreover ChIP experiments demonstrated that *PIL1* and *XTR7* are direct targets of PIF4 and PIF5 (de Lucas et al., 2008) (see below). Both genes were expressed at low levels in high R/FR in all genotypes. In response to low R/FR the expression of *PIL1* and *XTR7* was induced in all tested genotypes. In *pif4pif5* prolonged growth in low R/FR led to a reduced induction of their expression while in the *hfr1* mutant this induction was more pronounced than in the wild type (Figure 1B). Interestingly as for the growth response, the gene expression response of *hfr1pif4pif5* was more similar to the one of *pif4pif5* than *hfr1* (Figure 1B). *HFR1* expression is reduced in low R/FR-grown *pif4pif5* (Lorrain et al., 2008). In our conditions *HFR1* was expressed at about 50% of the wild-type levels (Supplementary Figure S1). The reduced expression of *HFR1* in *pif4pif5* can contribute but not fully explain the epistatic relationship observed here (see discussion).

Simulated shade leads to very rapid changes in the expression of shade marker genes (Salter et al., 2003; Sessa et al., 2005; Devlin et al., 2003) . This response is gated by the circadian clock (Devlin et al., 2003; Salter et al., 2003). We thus analyzed shade-induced changes in gene expression in seedlings that were synchronized by growth in a 12:12 day-night cycle. We followed the expression of *PIL1* and *XTR7* directly upon transfer from high to low R/FR conditions. Both *PIL1* and *XTR7* were rapidly induced in the wild type and the *hfr1* mutant. In the *hfr1* mutant the induction was somewhat more pronounced but the most striking feature was the previously reported reduced down-regulation of expression of those genes after prolonged exposure to low R/FR (Figure 2) (Sessa et al., 2005). The effect of HFR1 on shade-regulated gene expression is not as pronounced as what was reported previously (Sessa et al., 2005). This is most probably due to the different protocols used to study shade avoidance. We maintain PAR constant and only change the R/FR ratio while in a previous publication simulated shade conditions were obtained with a combination of red, blue and FR LED lights, which lead both to changes in PAR and R/FR ratio (Sessa et al., 2005). A direct comparison of the 2 protocols showed that they induce a somewhat different SAS for gene expression and hypocotyl elongation (data not shown). Consistent with our previous observations, the expression of *PIL1* and *XTR7* was markedly reduced in low R/FR grown *pif4pif5* double mutants (Figure 2) (Lorrain et

al., 2008). Importantly the *hfr1pif4pif5* triple mutant had essentially the same phenotype as *pif4pif5* (Figure 2). Interestingly the shade-induced expression of *IAA19* and *IAA29*, which depends on the TAA1 pathway, is still robustly induced in *pif4pif5* (Supplementary Figure S2). However the level of those genes was reduced in high R/FR grown *pif4pif5* and *hfr1pif4pif5* (Supplementary Figure S2). Finally, the same effects on shade-induced gene expression were observed when those genotypes were grown in continuous light prior to a change in light quality (Supplementary Figure S3). These genetic data lead us to hypothesize that HFR1 may inhibit PIF4 and PIF5 during the response to shade and thus limit the shade avoidance response particularly after a prolonged exposure to low R/FR.

HFR1 interacts with PIF4 and PIF5

bHLH class transcription factors work as homo- and/or heterodimers. Moreover it has been reported previously that HFR1 interacts with PIF3 *in vitro* and in the yeast two-hybrid assay (Fairchild et al., 2000). We thus tested whether HFR1 interacted with PIF4 and PIF5 by co-immunoprecipitation of *in vitro* transcribed and translated proteins. As a control for specificity we included a modified version of HFR1 (HFR1*), which contains a substitution of two conserved residues in the HLH domain (Val172 Leu173 to Asp172 Glu 173) (Supplementary Figure S4A). Based on a previous publication these substitutions are expected to interfere with the dimerization properties of the HLH domain (Voronova and Baltimore, 1990). Homology modeling of the wild-type and mutant versions of HFR1 supported this prediction (data not shown). Co-immunoprecipitation showed that HFR1 interacted with PIF4 and PIF5 while no specific binding of HFR1* to PIF4 or PIF5 was detected (Figure 3A,B). These data show that HFR1 specifically interacted with PIF4 and PIF5 and that this interaction critically depended on two residues in the HLH domain (Figure 3A,B).

To confirm this interaction in plant cells we used the Bimolecular Fluorescence Complementation (BIFC) assay in transiently transformed onion epidermal cells. The N and C-terminal halves of YFP were fused to the C-terminus of PIF4, PIF5, HFR1 and HFR1*. As a transformation control those cells were co-transformed with a soluble DsRed construct and DsRed positive cells were monitored for YFP fluorescence. HFR1 interacted with PIF4 and PIF5 in this assay and as expected the YFP fluorescence was detected in the nuclei of the transformed cells (Figure 3C). In

contrast cells transformed with HFR1* and either PIF4 or PIF5 were not YFP positive again indicating that those two conserved residues of the HFR1 HLH domain are important for dimerization (Figure 3C). Finally, co-immunoprecipitation using double transgenic lines carrying PIF5-HA and HFR1-Flag showed the interaction of HFR1 with PIF5 in Arabidopsis plants (Figure 3D).

HFR1 inhibits PIF5-mediated expression of *PIL1*

The facts that HFR1 and PIF4 / PIF5 had an opposite effect on the expression of shade marker genes and that these proteins dimerized raised the possibility that HFR1 may inhibit PIF-mediated gene expression by forming heterodimers. To test this possibility, we used a transient expression system with Arabidopsis cell cultures. We used 2 kb of the *PIL1* promoter containing 3 G-boxes fused the glucuronidase gene (*GUS*) as a reporter (Figure 4A). Effector constructs for PIF5, HFR1 and HFR1* were expressed under the control of the 2x*CaMV 35S* promoter and co-bombarded with the reporter construct and a transformation reference plasmid (2x*CaMV 35S* promoter:*LUC*) (Figure 4A). Transformation with PIF5 resulted in a strong stimulation of the *PIL1* reporter activity, which depended on the presence of the G-boxes in the promoter sequence (Figure 4B). This result is consistent with our genetic data indicating that PIF5 is a positive regulator of *PIL1* expression (Figures 1 and 2) (Lorrain et al., 2008). Transformation with HFR1 and HFR1* only had a minor effect on reporter expression (Figure 4C). The co-expression of PIF5 and HFR1 limited PIF5-mediated *PIL1* expression. Importantly co-transformation with HFR1* did not affect the transactivation activity of PIF5 (Figure 4C), strongly suggesting that HFR1 inhibits PIF5-mediated transcription by forming heterodimers. In agreement with this finding transgenic lines carrying HFR1* under the control of the 35S promoter did not complement the *hfr1* phenotype, whereas wild-type HFR1 slightly overcomplemented the *hfr1* phenotype (Supplementary Figure S4). These data confirm the functional importance of the HFR1 dimerization capacity.

HFR1 prevents PIF4 and PIF5 from binding a G-box sequence

Several possibilities could explain how HFR1 inhibits PIF-mediated expression of shade marker genes. HFR1-PIF heterodimers may be unable to bind DNA and/or such dimers could have reduced transactivation activity. Given that the basic domain of HFR1 is unusual and has been suggested to be incompatible with binding to a G-box

(Fairchild et al., 2000), we first tested whether PIF-HFR1 dimers are capable of binding to a piece of the *PIL1* promoter containing a G-box using homology modeling. Our analysis predicted binding of the PIF5 homodimer to the CACGTG G-box present in the *PIL1* promoter. The basic region of PIF5 made direct contact with the major groove of the DNA molecule at the level of the G-box centre (Supplementary Figure S5). Several important interactions were taking place between the PIF5 protein and the *PIL1* promoter. Glu266 made hydrogen bonds to the adenine ring that faces the T base of the CACGTG G-box, while Arg270 interacted with the backbone and the guanine ring of the first G of the G-box. In addition Arg267 and Arg269 made ionic interactions with the backbone of both the central CG bases of the G-box, and the PIF5 Glu266 side chain and the backbone of the DNA strand facing the CACGTG G-box, respectively. A structural model of the HFR1-DNA complex suggested that compared to PIF5-DNA several key protein-DNA interactions were either lost or unfavorable in HFR1-DNA. In the HFR1 homodimer or HFR1/PIF5 heterodimer, residues Glu266 and Arg270 in PIF5 are replaced by Arg143 and Asp147 in HFR1, respectively (Supplementary Figure S5). These drastic modifications inverse the charges of the corresponding residues and strongly diminish the possibility of interaction taking place between the protein and the G-box. In the model structures of the HFR1 homo- and heterodimer complexes to DNA, Asp147 did not make any contact with the promoter, while Arg143 made interactions with the backbone and the guanine ring of the first G base of the G-box. This modified scheme of interactions between PIF5 / DNA and HFR1 / DNA suggested that the HFR1-PIF5 heterodimer does not form a stable interaction with the G-box. Identical conclusions were reached by analyzing PIF4/PIF4 homodimers and PIF4/HFR1 heterodimers (data not shown).

To test these predictions biochemically we performed Electrophoretic Mobility Shift Assays (EMSA) with a fragment of the *PIL1* promoter containing the two closely spaced G-boxes (Figure 4A) and *in vitro* transcribed and translated HFR1, HFR1*, PIF4 and PIF5. PIF4 specifically bound to the G-box in the *PIL1* promoter, as demonstrated with competition experiments using wild-type and G-box mutant probes (Figure 5A) (Huq and Quail, 2002). Similar data were obtained for PIF5 except that two complexes of different sizes could be detected raising the possibility that PIF5 could simultaneously bind to both G-boxes in the DNA probe (Figure 5C). Finally

confirming our *in silico* predictions HFR1 was not able to bind to the *PIL1* promoter (Figure 5A, C lane 9). To test whether HFR1 could interfere with PIF4 and PIF5 DNA-binding, HFR1 and either PIF4 or PIF5 were co-produced by *in vitro* transcription/translation reactions and used for EMSA assays. These experiments showed that HFR1 inhibited the capacity of PIF4 and PIF5 to bind DNA (Figure 5B, D). Importantly when PIF4 and PIF5 were co-produced with HFR1* the non-heterodimerizing HFR1 variant did not interfere with PIF DNA-binding (Figure 5B, D). Equal protein production of the different bHLH proteins was verified by labeling the *in vitro* transcription translation reactions with ^{35}S Met (Supplementary Figure S6). Our biochemical experiments thus confirmed that HFR1 inhibits PIF4 and PIF5 from binding to the G-boxes in the *PIL1* promoter by forming non-DNA-binding heterodimers with those transcription factors. Importantly those G-boxes are required for PIF5-mediated *PIL1::GUS* expression (Figure 4B).

PIF5 directly binds to the G-box of shade marker genes *in vivo.*

Our data suggest that PIF4 and PIF5 regulate shade marker gene expression by directly binding to G-boxes present in those promoters (Figure 4). PIF4 has been shown to bind to the promoter of *PIL1* and *XTR7* (de Lucas et al., 2008). We analyzed binding of PIF5 to the promoters of *HFR1*, *XTR7* and *PIL1* by Chromatin ImmunoPrecipitation (ChIP) using plants constitutively expressing PIF5-HA (Lorrain et al., 2008). As controls we used wild type Col plants and HFR1-HA expressing plants. ChIP performed with an anti-HA epitope antibody was followed by Q-PCR to compare binding to part of the promoter containing a G-box with a part of the same gene devoid of a G-box. We found significant binding of PIF5-HA but not HFR1-HA (up to 1% of the input DNA on the *HFR1* promoter) specifically to the G-box containing fragment of *HFR1*, *PIL1* and *XTR7* (Figure 6). The fraction of DNA co-immunoprecipitated with PIF5-HA was consistently higher for *HFR1* than *XTR7* (Figure 6, data not shown). However in all three genes tested the difference between PIF5-HA and HFR1-HA was very large (Figure 6). Consistent with our in vitro experiments, these data indicate that PIF5-HA but not HFR1-HA directly bound to the G-box present in the promoter regions of *HFR1*, *PIL1* and *XTR7* (Figures 5 and 6).

Discussion

For shade-intolerant plants such as Arabidopsis a drop in the R/FR ratio signals the presence of competitors, which absorb red and blue light with their photosynthetic pigments. In response to this signal shaded plants adapt their morphology in order to reach direct sunlight. However, the SAS includes a negative feedback loop (e.g. HFR1, PAR1, PAR2) to prevent an exaggerated growth response (Roig-Villanova et al., 2007; Sessa et al., 2005). The mechanism of action of these three bHLH transcription factors was unknown. Our data provide a mechanistic understanding of a network of positively and negatively acting bHLH transcription factors involved in the response of plants to a signal from neighbors indicative of competition for light. Depending on the light conditions the phytochromes use two distinct mechanisms to control PIF activity. In conditions typical of sunlight PIF4 and PIF5 are rapidly degraded while in conditions typical of shade PIF4 and PIF5 remain stable but the HFR1 inhibitor is induced in a phytochrome-regulated manner (Lorrain et al., 2008; Sessa et al., 2005; Fairchild et al., 2000; Nozue et al., 2007; Duek and Fankhauser, 2003). This second mechanism is much slower than phytochrome-induced degradation (and potentially reversible), which thus leads to distinct windows of opportunity for PIF activity depending on the light condition.

The positive regulators of shade-induced growth PIF4 and PIF5 are rapidly stabilized in response to a reduction of the R/FR ratio (Lorrain et al., 2008). This contributes to the rapid induction of shade marker genes and elongation growth responses (Figures 1, 2) (Lorrain et al., 2008). Expression of those marker genes presumably depends directly on binding of PIF4 and PIF5 to G-boxes present in their promoters (Figure 4 and 6) (de Lucas et al., 2008). Here we show that HFR1 can dimerize with those PIFs and that these heterodimers are unable to bind to G-boxes present in the *PIL1* promoter (Figures 3 and 5). Consistent with this data co-expression of HFR1 and PIF5 in Arabidopsis cells inhibits PIF5-mediated expression of *PIL1:GUS* (Figure 4). bHLH class transcription factors are known to dimerize via their HLH domain (Voronova and Baltimore, 1990). We demonstrate the functional importance of HFR1's HLH domain in several ways. First a substitution of 2 amino acids in the HLH domain, which was shown to prevent dimerization of other HLH proteins, also prevented HFR1 from binding to PIF4 and PIF5 (Figure 3) (Voronova and Baltimore,

1990). Importantly this variant of HFR1 (HFR1*) was unable to prevent PIF4 and PIF5 from binding to DNA *in vitro* and PIF5 from promoting the expression from the *PIL1* promoter in Arabidopsis cells (Figures 4 and 5). Finally HFR1* was inactive *in vivo* as it could not complement the *hfr1* phenotype (Supplementary Figure S4). Taken together our results strongly support a model where HFR1 inhibits the shade avoidance response by forming non-DNA binding heterodimers with PIF4 and PIF5. This model predicts that HFR1 acts through PIF4 and PIF5 and thus that *pif4pif5* should be epistatic over *hfr1*, which is largely consistent with our genetic analysis (Figures 1 and 2). This is particularly clear for the rapid light effects on gene expression (Figure 2 and S3), while after a prolonged treatment in the shade *pif4pif5* is not fully epistatic over *hfr1* (Figure 1). One possible interpretation of this result is that HFR1 could also inactivate additional PIF proteins, such as PIF3, which was shown to interact with HFR1 *in vitro* (Fairchild et al., 2000). An alternative explanation for the genetic interactions reported here would be that in *pif4pif5* mutants *HFR1* is no longer expressed. Consistent with our previous results HFR1 expression is reduced in the *pif4pif5* double mutant, however it was still at 50% of the wild-type level in the double mutant (Supplementary Figure S1) (Lorrain et al., 2008). We thus conclude that it is unlikely that this reduction in *HFR1* expression in *pif4pif5* plants fully explains our genetic interactions.

Interestingly *HFR1* is also induced in a PIF-dependent manner when plants perceive low R/FR and PIF5 directly binds to the *HFR1* promoter (Figures 6 and S1) (Lorrain et al., 2008). Thus a negative regulator of the shade avoidance response is an early responsive gene, which is typical for negative feedback loops. The pattern of *HFR1* expression may at least in part explain the transient up-regulation of many shade marker genes. In the early phase of the response to shade the response is dominated by the stabilization of PIF4 and PIF5 while at later stages the increased expression of *HFR1* limits their activity. This model is fully consistent with the greater influence of HFR1 on the later stages of low R/FR-regulated gene expression (Figure 2) (Sessa et al., 2005). It should however also be noted that the transient upregulation of shade maker genes is also partly due to gating of the shade avoidance response by the circadian clock (Salter et al., 2003). Interestingly *PIF4* and *PIF5* expression are under circadian regulation, which may directly contribute to gating of the SAS (Nozue et al., 2007).

While our model is fully consistent with our results the phenotype of the *pif4pif5* double mutant also shows that other important mechanism contribute to shade-induced growth (Figures 1, 2 and S3) (Lorrain et al., 2008). Indeed the *pif4pif5* double mutant still displays a robust induction of hypocotyl growth in response to a reduction of the R/FR ratio (Figure 1) (Lorrain et al., 2008). We thus propose that in response to a drop in the R/FR ratio multiple mechanisms are coordinately implemented in order to ensure a robust response. The rapid increase in TAA1-mediated auxin biosynthesis is certainly one of them (Tao et al., 2008). Interestingly in the *sav3/taa1* mutant several early shade marker genes including *HFR1*, *ATHB2* and *RIP* are still normally induced while expression of those genes strongly depends on PIF4 and PIF5 (Figures 1, 2, data not shown) (Lorrain et al., 2008; Tao et al., 2008) In contrast, the induction by shade of several auxin-regulated transcripts, which depend on the TAA1-pathway is only marginally affected in *pif4pif5* (Supplementary Figure S2). These results suggest that at least two pathways can be activated independently. While the PIF4, PIF5 and HFR1 network that we describe largely explains the transcriptional regulation of shade-regulated genes, the mechanism by which TAA1 is activated by shade is currently unknown but *TAA1* transcript levels do not increase in response to a drop in the R/FR ratio (Tao et al., 2008). Interestingly, both SAV3/TAA1 and PIF4 are not only required to promote growth in response to shade but also in response to elevated temperatures (Koini et al., 2009; Tao et al., 2008).

The mechanism of HFR1 action that we describe here is comparable to the one that was recently described for the DELLA proteins, which also inhibit PIF proteins by heterodimerization (Alabadi et al., 2008; Feng et al., 2008; de Lucas et al., 2008). Interestingly, DELLA proteins have also been implicated in the response of plants to shade (Djakovic-Petrovic et al., 2007). However the interplay between DELLA and PIF proteins during shade avoidance is currently unknown. In both cases the HLH domain of the PIFs has been implicated as the site of dimerization suggesting that depending on the conditions either HFR1 or the DELLA proteins will predominantly down-regulate PIF activity. Our genetic data indicate that during the response to a drop in the R/FR ratio HFR1 plays a predominant role in preventing excessive PIF activity. Moreover we have recently shown that PIF4 and PIF5 are also required during the de-etiolation phase of seedlings grown under continuous FR light (the FR-

HIR) (Lorrain et al., 2009). The genetic interaction between *hfr1* and *pif4pif5* indicates that under these conditions as well HFR1 acts by inhibiting PIF4 and PIF5 because *pif4pif5* is fully epistatic over *hfr1* (Lorrain et al., 2009). The strong expression of *HFR1* during the FR-HIR and during shade avoidance is consistent with a predominant function of HFR1 under these conditions while in high R/FR *HFR1* expression is low and *hfr1* mutants have no obvious phenotype (Figure 1) (Sessa et al., 2005; Fairchild et al., 2000; Duek and Fankhauser, 2003) . The DELLA proteins may primarily inhibit PIF proteins under conditions where HFR1 levels are low such as in darkness and in high R/FR light. This hypothesis is consistent with the reduced growth of the hypocotyls in etiolated seedlings with a reduced GA content (Alabadi et al., 2008). Low GA stabilizes the DELLAs, which could then inhibit PIF activity, which is required for normal etiolated development (Leivar et al., 2008; Shin et al., 2009; Stephenson et al., 2009).

bHLH proteins are capable of interacting with transcription factors from other families. In plants this has been particularly well documented during the control of trichrome development where bHLH class and MYB class transcription factors form a regulatory complex involved in cell fate determination (Zhao et al., 2008). Interestingly HFR1 has recently been shown to interact with the R2R3-MYB factor LAF1 (Jang et al., 2007). The heterodimerization of these two transcription factors leads to mutual stabilization of the two proteins. Somewhat surprisingly however genetic analysis suggests that LAF1 and HFR1 act largely independently during the FR-HIR (Jang et al., 2007). Moreover it is currently unknown whether this protein interaction has any effect on the DNA-binding capacity of those transcription factors. Mechanistically more related to the PIF-HFR1 regulatory network described here is the finding that Arabidopsis bHLH048 can inhibit DNA-binding of an unrelated class of transcription factor. However, the biological consequences of this interaction remain unknown (Husbands et al., 2007).

Previous studies in animals identified HLH proteins, such as ID (Inhibitor of DNA binding), which upon dimerization with bHLH proteins leads to the formation of non-DNA binding heterodimers (Norton, 2000). In contrast to ID proteins HFR1 possesses a basic domain just N-terminal of the HLH domain but their mode of action appears to be analogous. Interestingly ID proteins have recently been implicated in circadian

processes in mice potentially acting though the bHLH proteins BMAL1 and CLOCK (Duffield et al., 2009). Given that HFR1 inhibits PIF4 and PIF5, which are also required for the circadian-regulated plant growth, there might be a related regulatory network of HLH proteins controlling circadian responses in plants and animals (Duffield et al., 2009; Niwa et al., 2009; Nozue et al., 2007). The small HLH proteins PAR1 and PAR2 are negative regulators of the shade avoidance response, which may also act by preventing other bHLH proteins from binding to DNA (Roig-Villanova et al., 2007). Similarly the regulator of hypocotyl growth KIDARI has also been proposed to act like ID proteins (Hyun and Lee, 2006). HFR1 and KIDARI regulate hypocotyl elongation in opposite ways and both proteins interact *in vitro*, raising the possibility that by sequestering HFR1, KIDARI may promote PIF-mediated growth. However to the best of our knowledge HFR1 is the first plant bHLH protein for which there is a direct demonstration that it acts by inhibiting DNA binding of other bHLH proteins (PIF4 and PIF5). Future work will determine whether HFR1 can also interfere with other members of the PIF family by heterodimerization. The finding that a stabilized version of HFR1 leads to a constitutively photomorphogenic phenotype similar to the one reported for *pif1pif3pif4pif5* quadruple mutants is certainly consistent with this idea (Leivar et al., 2008; Shin et al., 2009; Stephenson et al., 2009; Yang et al., 2003) .

Materials and methods

Plant material and growth conditions

Seeds of *Arabidopsis thaliana*, ecotype Columbia, were surface sterilized and either plated on 1/2 strength MS, 0.7% phytagar (Murashige and Skoog medium, GIBCO 23118-037) or directly onto soil. After 3 days at 4°C, plants were grown at 22°C in a Percival Scientific Model I-66L with or without supplementary far-red (λmax 739 nm; Quantum Device, USA) diodes. Fluence rates were determined with an International light IL1400A photometer equipped with an SEL033 probe with appropriate light filters. The ratios of R/FR were the following, high=17, low=0.25. PAR was constant at 60 µmol m^{-2} s^{-1}. The double mutant *pif4pif5* has been described previously (Lorrain et al., 2008). The triple mutant was obtained by crossing the *pif4pif5* double mutant with *hfr1-101* and genotyping was performed as described previously (Duek and Fankhauser, 2003; Lorrain et al., 2008). Hypocotyl length measurement was achieved using imageJ software.

To generate plants expressing tagged versions of PIF5 and HFR1 we transformed PIF5-HA expressing plants (Lorrain et al., 2008) with a construct coding for HFR1 with a triple Flag tag under the control of the cauliflower mosaic virus promoter 35S. A Flag-tagged HFR1 was generated by PCR using the primers pSP05 and pPH24 with the full length HFR1 cDNA as a template. The PCR product was digested with KpnI and SacI and introduced into pSL35 (pBSIISK+ (Invitrogen) containing a triple Flag tag) to generate pSL30. HFR1-3xFlag was then sub-cloned into the pCHF6 binary vector to generate pSL33. This construct was transformed into PIF5-3xHA overexpressing Arabidopsis plants by the *Agrobacterium* dipping method. Transformants with a 3:1 segregation ratio were self-fertilized, and homogenous progeny were selected. Primer sequences are given on supplementary table I.

Analysis of gene expression

RNA extraction was performed using the kit Nucleo Spin for plant RNA from Machery-Nagel and reverse-transcribed using the SuperScript II Reverse Transcriptase (Invitrogen) according to the manufacturer's instructions. Q-PCR was

performed with the Power SYBR Green PCR master mix from Applied Biosystems using the ABI Prism 7900HT Sequence Detection Systems (Applied Biosystems) according to the manufacturer's instructions. For the relative quantification of the genes qBase, a software for management and automated analysis of real-time Q-PCR data was used (http://medgen.ugent.be/qbase). Each reaction was performed in triplicate using a primer concentration of 300 nM. Quantitative PCR were performed using the primer pairs pPH49/pPH50 (*PIL1*: At2G46970), Mt121/Mt122 (*XTR7:* At4G14130), SL44/SL45 (*HFR1:* At1G02340), Mt123/Mt124 (*IAA19:* At3G15540), Mt157/Mt158 (*IAA29* At4G32280), F_*EF1α*/R_*EF1α* (*EF1α:* At5G60390) and F_*GAPC-2*/R_*GAPC-2* (*GAPC-2* A1G13440). Primer sequences are given on supplementary table I.

In vitro co-immunoprecipitation

Proteins were synthesized in the reticulocyte TNT *in vitro* transcription/translation system (Promega) and labeled with ^{35}S-methionine according to the manufacturer's instructions. The full-length HFR1 cDNA was cloned with BamHI linkers into pCMX-PL1. HFR1* was generated by site directed mutagenesis using the primers pPH20 and pPH21 using the QuikChange Site-Directed Mutagenesis Kit from Stratagene. PIF4-3xHA was inserted with KpnI and NheI into PCMX-PL1 and PIF5-3xHA was inserted with KpnI and NheI into PCMX-PL2. All constructs were verified by sequencing. Proteins were incubated with HA-antibodies coupled to agarose beads (Anti-HA Affinity Matrix; Roche) in binding buffer (25 mM Hepes pH 7.5, 100 mM KCl, 0.2 mM EDTA, 10% glycerol, 2.5 mM $MgCl_2$, 1 mM DTT, 0.5% NP-40 and SIGMA protease inhibitor 10 ul/ml). The beads were washed five times with the binding buffer. Specifically bound proteins were eluted with Laemmli buffer (immunoprecipitation = IP). IP and input fractions were separated on 10% SDS-PAGE gels and visualized using a phosphorimager.

Bimolecular fluorescence complementation (BiFC) assays

Genes were cloned under the control of the 35S promoter and fused to either the C- or N-terminal part of YFP. HFR1/HFR1* were cloned into the XbaI-XhoI sites of pUC-SPYNE (Walter et al., 2004). PIF4 was cloned XbaI-XhoI into pUC-SPYCE and PIF5 was cloned SpeI-XhoI into pUC-SPYCE (Walter et al., 2004). The resulting

constructs were mixed as indicated (800 ng each) and co-bombarded into onion cells. DNA precipitation and particle bombardement was performed using the Biorad helium-driven particle accelerator (PDS-1000) according to the manufacturer's instructions. Onions were kept in the dark for 16 h at 22°C to allow expression of the transfected DNA and reconstruction of the functional YFP. All fluorescence microscopy was performed using Leica DM6000B microscope.

In vivo co immumoprecipitation

10 mg of seeds were plated in Petri dishes and stored in the dark for 3 days at 4°C. A germinating red light treatment was given at 22°C and the plates returned to darkness for further three days. Plates were then transferred to white light with high R/FR ratio for 1h30 and then in white light with a low R/FR for additional 2h30 before protein extraction. Seedlings were ground in cold mortar with protein extraction buffer (50mM Tris. HCl pH7.5; 100mM NaCl; 10% glycerol; 0.1% NP-40; 1mM DTT; 1x protease inhibitors (SIGMA); 50µM MG132). Soluble proteins were incubated with 40µL of EZview red anti FlagM2 affinity gel (SIGMA) beads for 1h30 at 4°C. After 4 washes in the protein extraction buffer, specifically-bound proteins were eluted with Laemmli buffer. HRP-conjugated anti-HA antibodies (Roche) or Anti Flag M2 antibodies (SIGMA) and HRP-conjugated anti mouse antibodies (Promega) were used to detect proteins.

Transactivation assay

The transactivation assays were performed as previously described (de Lucas et al., 2008). The effector constructs carry PIF5 or HFR1/HFR1* under the control of the 2x*35S* promoter. The reporter construct carries the *GUS* gene driven by 2 kb of the *PIL1* promoter, which was amplified using the primers pPH017 and pPH09. The triple G-box mutant of *pPIL1* (p*PIL1**::GUS) was generated by site directed mutagenesis using the QuikChange Site-Directed Mutagenesis Kit from Stratagene. The double G-Box was mutated using the primers pPH45 and pPH46 and the single G-Box using the primers pPH47 and pPH48. A *2x35S*::luciferase construct was used as an internal control. Three independent experiments were carried out with three biological replica plates for each treatment.

Electrophoresis mobility shift assays (EMSA)

Proteins were synthesized using the TNT system (Promega). To produce PIF4 protein full-length PIF4 cDNA was cloned into pCMX-PL1. Two PIF4 fragments (BclI/ NcoI, NcoI / KpnI) were inserted via a three-way ligation. Full-length PIF5 cDNA was cloned with KpnI and NheI into pCXM-PL2. For the DNA probe single stranded primers were 5' labeled with radioactive γ-phosphate of ATP (γ^{32}P) using polynucleotide kinase (PNK). Forward and reverse primers FGbox / RGbox or FGbox-Mt / RGbox-Mt were annealed and purified using the Quick Spin Column (Roche). The binding reactions were performed according to (Martinez-Garcia et al., 2000). The binding complexes (45 000 cpm per reaction) were resolved on a 6% polyacrylamide gel and visualized using a phosphorimager.

Chromatin immunoprecipitation (ChIP) and PCR amplification

Arabidopsis thaliana seeds (Col, 35S::HFR1-3xHA (CF396) (Duek et al 2004) and 35S::PIF5-3xHA (Lorrain et al 2008)) were plated on 1/2 strength MS, 0.7% phytagar. After 3 days at 4°C, seedlings were grown in long-day conditions at 22°C. 10-day-old seedlings were shifted 2 hours into low R/FR before fixation. Chromatin immunoprecipitation assays were performed as described previously (Pruneda-Paz et al., 2009). Immunoprecipitation was performed with HA-antibodies coupled to agarose beads (Anti-HA Affinity Matrix; Roche) and immunocomplexes were eluted from the beads using elution buffer (0.1M NaHCO3, 1% SDS). DNA was purified with the GenElute PCR Clean up Kit from SIGMA and used for the quantification of immunoprecipitated DNA by Q-PCR. Each Q-PCR reaction was performed in triplicate. The forward and reverse primer pairs used to amplify the region 1-6 are the following: *PIL1*-region 1 (pPH78-pPH79), *PIL1*-region 2 (pPL8F-pPL8R), *XTR7*-region 3 (pPH120-pPH121), *XTR7*-region 4 (pPH130- pPH131), *HFR1*-region 5 (pPH112-pPH113) and *HFR1*-region 6 (pPH126- pPH127). Primer sequences are given on supplementary table I.

Supplementary data

Supplementary data are available at The EMBO Journal
Online (http://www.embojournal.org).

Acknowledgements

We thank Manuel Bueno for advice for Q-PCR, Céline Wyser and Martine Trevisan for technical support and Frédéric Schütz (SIB) for advice on statistics. We are grateful to the Protein Modeling Facility (PMF, Lausanne University) and the DNA-array facility (DAFL http://www.unil.ch/dafl) for their help during this work. We thank Jörg Kudla (University of Münster) for providing the BiFC vectors. We thank Keara Franklin (University of Leicester) for critical reading of this manuscript. This work was supported by grants from the Swiss National Science Foundation (3100A0-112638 and 31003A_124747/1) to C.F., a short-term Roche doctoral fellowship (225-2008) to P.H. and the University of Lausanne.

Figure legends

Figure 1: The *pif4pif5* mutations are largely epistatic over *hfr1* in long-term shade conditions.

Seedlings were grown for 8.5 days in high R/FR (white bars) or for 4 days in high R/FR followed by 4.5 days in low R/FR (black bars).

(A) Hypocotyl length measurements, data are the mean, error bars represent 2xSE, n=15. **(B)** Gene expression of *PIL1* and *XTR7* was determined by Q-PCR analysis. Biological triplicates were performed with technical triplicates for each sample. Values were normalized with *EF1α* and *GAPC-2*. Relative expressions to Col-0 in high R/FR is shown. Error bars represent SE of the biological triplicates.

Figure 2: The *pif4pif5* mutations are epistatic over *hfr1* in early-responses to shade.

Seedlings were grown for 6 days in high R/FR (12 h light / 12h dark) and then either kept in high R/FR ratios or shifted to low R/FR ratios.

The expression of *PIL1* and *XTR7* was analyzed by Q-PCR. Three technical replicas were performed for each sample. Values were normalized with *EF1α* and *GAPC-2*. Relative expressions to Col-0 (point 0) are shown. Error bars represent SE of the technical triplicates.

Figure 3: HFR1 interacts with PIF4 and PIF5.

(**A**, **B**) Co-immunoprecipitation of *in vitro* transcribed and translated proteins (^{35}S-Met labeled). The HA-tag was used for immunoprecipitation of PIF4 (**A**) or PIF5 (**B**) using HA-antibodies coupled to agarose beads. Proteins were separated by SDS-PAGE and visualized by autoradiography. (Immunoprecipitation = IP). (**C**) Bimolecular fluorescence complementation (BiFC) with HFR1 / HFR1* with PIF4 or PIF5 in plant cells. Onion cells were co-bombarded with N- and C-YFP fusion proteins. 1/3/5/7 dsRED signal of transfected cells; 2/4/6/8 YFP channel; Scale bar = 100 µm. (**D**) Co-immunoprecipitation of HFR1-Flag and PIF5-HA. 35S::HFR1-3xFlag (HFR1-Flag), 35S::PIF5-3xHA (PIF5-HA) and seedlings expressing both transgenes (HFR1-Flag and PIF5-HA) were grown for 3 days in the dark. After 2h30 in low R/FR proteins were extracted and co-immunoprecipitated using anti-Flag

antibodies. Proteins were separated by SDS-PAGE, western blotted and detected using antibodies raised against HA and Flag.

Figure 4: HFR1 inhibits PIF5 transactivation activity in Arabidopsis cells.

(A) Schematic presentation of the constructs including the positions of the 3 G-boxes present in the *PIL1* promoter. (**B**) Arabidopsis cells were co-bombarded with the *pPIL1::GUS* or *pPIL1*::GUS* in which the 3 G-boxes were mutated and either a vector control or PIF5. The transactivation activity of the effectors is given with the GUS values normalized to luciferase activity (the internal transfection control). Values are mean of three different transfections +/- SE. **(C**) Arabidopsis cells were co-bombarded with the *pPIL1::GUS* construct and combinations of the different effector constructs as indicated on the figure. The transactivation activity is calculated as in panel B.

Figure 5: HFR1 prevents PIF4 and PIF5 from binding to the G-box DNA sequence.

Electromobility shift assays (EMSA) in (**A-D**) were performed using *in vitro* transcribed and translated proteins and a ^{32}P-radiolabed DNA probe of the *PIL1* promoter sequence containing a double G-box. (**A**, **C**) The DNA probe (lane 1-9) was incubated with TNT master mix (lane 1) or PIF4 (**A**)/ PIF5 (**C**) with increasing amounts of unlabeled probe (lane 3-5) or mutated unlabeled probe (lane 6-8). Lane 9 contains HFR1. **(B**, **D**): Lane 1: PIF4 or PIF5 alone; Lane 2: PIF4 or PIF5 with HFR1; Lane 3: PIF4 or PIF5 with HFR1*. The arrow indicates the specific PIF-DNA complex. FP= Free probe

Figure 6: PIF5-HA but not HFR1-HA binds to the promoter of shade-induced genes *in vivo*.

Chromatin ImmunoPrecipitation (ChIP) from 12-day-old Col, 35S::HFR1-3xHA (HFR1) and 35S::PIF5-3xHA (PIF5) seedlings. (**A**) Schematic representation of the *PIL1*, *XTR7* and *HFR1* genes, including the regions amplified following ChIP and the position of G-boxes. (**B**) Immunoprecipitated DNA was quantified by Q-PCR using primers in the promoter region containing G-boxes (region 1, 3 and 5) or control regions without G-boxes (region 2, 4 and 6). Data are average of technical triplicates of the Q-PCR +/- SD. Data from one representative ChIP experiment is shown.

References

Alabadi, D. and Blazquez, M.A. (2009) Molecular interactions between light and hormone signaling to control plant growth. *Plant Mol Biol*, **69**, 409-417.

Alabadi, D., Gallego-Bartolome, J., Orlando, L., Garcia-Carcel, L., Rubio, V., Martinez, C., Frigerio, M., Iglesias-Pedraz, J.M., Espinosa, A., Deng, X.W. and Blazquez, M.A. (2008) Gibberellins modulate light signaling pathways to prevent Arabidopsis seedling de-etiolation in darkness. *Plant J*, **53**, 324-335.

Ballare, C.L. (1999) Keeping up with the neighbours: phytochrome sensing and other signalling mechanisms. *Trends Plant Sci*, **4**, 97-102.

Carabelli, M., Morelli, G., Whitelam, G. and Ruberti, I. (1996) Twilight-zone and canopy shade induction of the Athb-2 homeobox gene in green plants. *Proc Natl Acad Sci U S A*, **93**, 3530-3535.

Carabelli, M., Possenti, M., Sessa, G., Ciolfi, A., Sassi, M., Morelli, G. and Ruberti, I. (2007) Canopy shade causes a rapid and transient arrest in leaf development through auxin-induced cytokinin oxidase activity. *Genes Dev*, **21**, 1863-1868.

de Lucas, M., Daviere, J.M., Rodriguez-Falcon, M., Pontin, M., Iglesias-Pedraz, J.M., Lorrain, S., Fankhauser, C., Blazquez, M.A., Titarenko, E. and Prat, S. (2008) A molecular framework for light and gibberellin control of cell elongation. *Nature*, **451**, 480-484.

Devlin, P.F., Patel, S.R. and Whitelam, G.C. (1998) Phytochrome E influences internode elongation and flowering time in Arabidopsis. *Plant Cell*, **10**, 1479-1487.

Devlin, P.F., Robson, P.R., Patel, S.R., Goosey, L., Sharrock, R.A. and Whitelam, G.C. (1999) Phytochrome D acts in the shade-avoidance syndrome in Arabidopsis by controlling elongation growth and flowering time. *Plant Physiol*, **119**, 909-915.

Devlin, P.F., Yanovsky, M.J. and Kay, S.A. (2003) A genomic analysis of the shade avoidance response in Arabidopsis. *Plant Physiol*, **133**, 1617-1629.

Djakovic-Petrovic, T., de Wit, M., Voesenek, L.A. and Pierik, R. (2007) DELLA protein function in growth responses to canopy signals. *Plant J*, **51**, 117-126.

Duek, P.D. and Fankhauser, C. (2003) HFR1, a putative bHLH transcription factor, mediates both phytochrome A and cryptochrome signalling. *Plant J*, **34**, 827-836.

Duffield, G.E., Watson, N.P., Mantani, A., Peirson, S.N., Robles-Murguia, M., Loros, J.J., Israel, M.A. and Dunlap, J.C. (2009) A role for Id2 in regulating photic entrainment of the mammalian circadian system. *Curr Biol*, **19**, 297-304.

Fairchild, C.D., Schumaker, M.A. and Quail, P.H. (2000) HFR1 encodes an atypical bHLH protein that acts in phytochrome A signal transduction. *Genes Dev*, **14**, 2377-2391.

Feng, S., Martinez, C., Gusmaroli, G., Wang, Y., Zhou, J., Wang, F., Chen, L., Yu, L., Iglesias-Pedraz, J.M., Kircher, S., Schafer, E., Fu, X., Fan, L.M. and Deng, X.W. (2008) Coordinated regulation of Arabidopsis thaliana development by light and gibberellins. *Nature*, **451**, 475-479.

Franklin, K.A. (2008) Shade avoidance. *New Phytol*, **179**, 930-944.

Franklin, K.A. and Whitelam, G.C. (2005) Phytochromes and shade-avoidance responses in plants. *Ann Bot (Lond)*, **96**, 169-175.

Hisamatsu, T., King, R.W., Helliwell, C.A. and Koshioka, M. (2005) The involvement of gibberellin 20-oxidase genes in phytochrome-regulated petiole elongation of Arabidopsis. *Plant Physiol*, **138**, 1106-1116.

Huq, E. and Quail, P.H. (2002) PIF4, a phytochrome-interacting bHLH factor, functions as a negative regulator of phytochrome B signaling in Arabidopsis. *Embo J*, **21**, 2441-2450.

Husbands, A., Bell, E.M., Shuai, B., Smith, H.M. and Springer, P.S. (2007) LATERAL ORGAN BOUNDARIES defines a new family of DNA-binding transcription factors and can interact with specific bHLH proteins. *Nucleic Acids Res*, **35**, 6663-6671.

Hyun, Y. and Lee, I. (2006) KIDARI, encoding a non-DNA Binding bHLH protein, represses light signal transduction in Arabidopsis thaliana. *Plant Mol Biol*, **61**, 283-296.

Izaguirre, M.M., Mazza, C.A., Biondini, M., Baldwin, I.T. and Ballare, C.L. (2006) Remote sensing of future competitors: impacts on plant defenses. *Proc Natl Acad Sci U S A*, **103**, 7170-7174.

Jang, I.C., Yang, S.W., Yang, J.Y. and Chua, N.H. (2007) Independent and interdependent functions of LAF1 and HFR1 in phytochrome A signaling. *Genes Dev*, **21**, 2100-2111.

Kanyuka, K., Praekelt, U., Franklin, K.A., Billingham, O.E., Hooley, R., Whitelam, G.C. and Halliday, K.J. (2003) Mutations in the huge Arabidopsis gene BIG affect a range of hormone and light responses. *Plant J*, **35**, 57-70.

Koini, M.A., Alvey, L., Allen, T., Tilley, C.A., Harberd, N.P., Whitelam, G.C. and Franklin, K.A. (2009) High temperature-mediated adaptations in plant architecture require the bHLH transcription factor PIF4. *Curr Biol*, **19**, 408-413.

Kurepin, L.V., Emery, R.J., Pharis, R.P. and Reid, D.M. (2007a) The interaction of light quality and irradiance with gibberellins, cytokinins and auxin in regulating growth of Helianthus annuus hypocotyls. *Plant Cell Environ*, **30**, 147-155.

Kurepin, L.V., Emery, R.J., Pharis, R.P. and Reid, D.M. (2007b) Uncoupling light quality from light irradiance effects in Helianthus annuus shoots: putative roles for plant hormones in leaf and internode growth. *J Exp Bot*, **58**, 2145-2157.

Leivar, P., Monte, E., Oka, Y., Liu, T., Carle, C., Castillon, A., Huq, E. and Quail, P.H. (2008) Multiple phytochrome-interacting bHLH transcription factors repress premature seedling photomorphogenesis in darkness. *Curr Biol*, **18**, 1815-1823.

Lorrain, S., Allen, T., Duek, P.D., Whitelam, G.C. and Fankhauser, C. (2008) Phytochrome-mediated inhibition of shade avoidance involves degradation of growth-promoting bHLH transcription factors. *Plant J*, **53**, 312-323.

Lorrain, S., Trevisan, M., Pradervand, S. and Fankhauser, C. (2009) Phytochrome interacting factors 4 and 5 redundantly limit seedling de-etiolation in continuous far-red light. *Plant J. Accepted Article Online: Jul 8 2009 DOI: 10.1111/j.1365-313X.2009.03971.x*

Martinez-Garcia, J.F., Huq, E. and Quail, P.H. (2000) Direct targeting of light signals to a promoter element-bound transcription factor. *Science*, **288**, 859-863.

Morelli, G. and Ruberti, I. (2002) Light and shade in the photocontrol of Arabidopsis growth. *Trends Plant Sci*, **7**, 399-404.

Moreno, J.E., Tao, Y., Chory, J. and Ballare, C.L. (2009) Ecological modulation of plant defense via phytochrome control of jasmonate sensitivity. *Proc Natl Acad Sci U S A*, **106**, 4935-4940.

Niwa, Y., Yamashino, T. and Mizuno, T. (2009) Circadian Clock Regulates Photoperiodic Response of Hypocotyl Elongation through a Coincidence Mechanism in Arabidopsis thaliana. *Plant Cell Physiol*.

Norton, J.D. (2000) ID helix-loop-helix proteins in cell growth, differentiation and tumorigenesis. *J Cell Sci*, **113 (Pt 22)**, 3897-3905.

Nozue, K., Covington, M.F., Duek, P.D., Lorrain, S., Fankhauser, C., Harmer, S.L. and Maloof, J.N. (2007) Rhythmic growth explained by coincidence between internal and external cues. *Nature*, **448**, 358-361.

Pruneda-Paz, J.L., Breton, G., Para, A. and Kay, S.A. (2009) A functional genomics approach reveals CHE as a component of the Arabidopsis circadian clock. *Science*, **323**, 1481-1485.

Roig-Villanova, I., Bou-Torrent, J., Galstyan, A., Carretero-Paulet, L., Portoles, S., Rodriguez-Concepcion, M. and Martinez-Garcia, J.F. (2007) Interaction of shade avoidance and auxin responses: a role for two novel atypical bHLH proteins. *Embo J*, **26**, 4756-4767.

Salter, M.G., Franklin, K.A. and Whitelam, G.C. (2003) Gating of the rapid shade-avoidance response by the circadian clock in plants. *Nature*, **426**, 680-683.

Sessa, G., Carabelli, M., Sassi, M., Ciolfi, A., Possenti, M., Mittempergher, F., Becker, J., Morelli, G. and Ruberti, I. (2005) A dynamic balance between gene activation and repression regulates the shade avoidance response in Arabidopsis. *Genes Dev*, **19**, 2811-2815.

Shen, Y., Khanna, R., Carle, C.M. and Quail, P.H. (2007) Phytochrome induces rapid PIF5 phosphorylation and degradation in response to red-light activation. *Plant Physiol*, **145**, 1043-1051.

Shin, J., Kim, K., Kang, H., Zulfugarov, I.S., Bae, G., Lee, C.H., Lee, D. and Choi, G. (2009) Phytochromes promote seedling light responses by inhibiting four negatively-acting phytochrome-interacting factors. *Proc Natl Acad Sci U S A*, **106**, 7660-7665.

Sorin, C., Salla-Martret, M., Bou-Torrent, J., Roig-Villanova, I. and Martinez-Garcia, J.F. (2009) ATHB4, a regulator of shade avoidance, modulates hormone response in Arabidopsis seedlings. *Plant J*, **59**, 266-277.

Stepanova, A.N., Robertson-Hoyt, J., Yun, J., Benavente, L.M., Xie, D.Y., Dolezal, K., Schlereth, A., Jurgens, G. and Alonso, J.M. (2008) TAA1-mediated auxin biosynthesis is essential for hormone crosstalk and plant development. *Cell*, **133**, 177-191.

Stephenson, P.G., Fankhauser, C. and Terry, M.J. (2009) PIF3 is a repressor of chloroplast development. *Proc Natl Acad Sci U S A*, **106**, 7654-7659.

Tanaka, S., Nakamura, S., Mochizuki, N. and Nagatani, A. (2002) Phytochrome in cotyledons regulates the expression of genes in the hypocotyl through auxin-dependent and -independent pathways. *Plant Cell Physiol*, **43**, 1171-1181.

Tao, Y., Ferrer, J.L., Ljung, K., Pojer, F., Hong, F., Long, J.A., Li, L., Moreno, J.E., Bowman, M.E., Ivans, L.J., Cheng, Y., Lim, J., Zhao, Y., Ballare, C.L., Sandberg, G., Noel, J.P. and Chory, J. (2008) Rapid synthesis of auxin via a new tryptophan-dependent pathway is required for shade avoidance in plants. *Cell*, **133**, 164-176.

Vandenbussche, F., Pierik, R., Millenaar, F.F., Voesenek, L.A. and Van Der Straeten, D. (2005) Reaching out of the shade. *Curr Opin Plant Biol*, **8**, 462-468.

Voronova, A. and Baltimore, D. (1990) Mutations that disrupt DNA binding and dimer formation in the E47 helix-loop-helix protein map to distinct domains. *Proc Natl Acad Sci U S A*, **87**, 4722-4726.

Walter, M., Chaban, C., Schutze, K., Batistic, O., Weckermann, K., Nake, C., Blazevic, D., Grefen, C., Schumacher, K., Oecking, C., Harter, K. and Kudla, J. (2004) Visualization of protein interactions in living plant cells using bimolecular fluorescence complementation. *Plant J*, **40**, 428-438.

Yang, K.Y., Kim, Y.M., Lee, S., Song, P.S. and Soh, M.S. (2003) Overexpression of a mutant basic helix-loop-helix protein HFR1, HFR1-deltaN105, activates a branch pathway of light signaling in Arabidopsis. *Plant Physiol*, **133**, 1630-1642.

Zhao, M., Morohashi, K., Hatlestad, G., Grotewold, E. and Lloyd, A. (2008) The TTG1-bHLH-MYB complex controls trichome cell fate and patterning through direct targeting of regulatory loci. *Development*, **135**, 1991-1999.

Figure 1

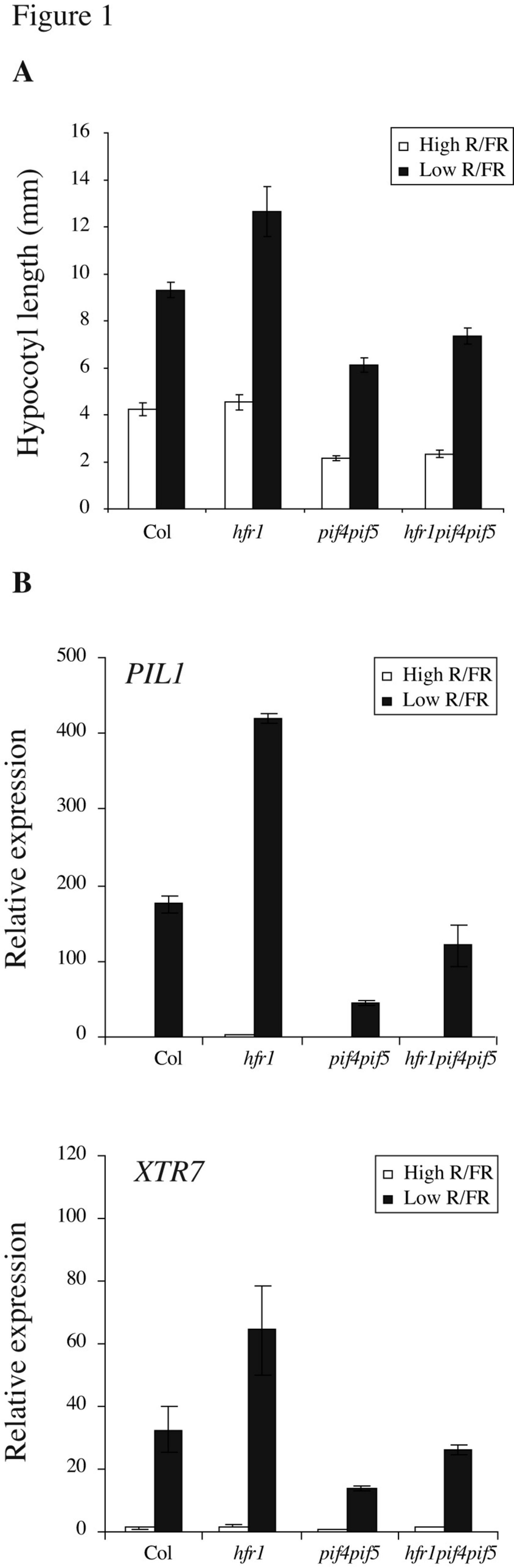
A
Hypocotyl length (mm)
16
14
12
10
8
6
4
2
0
High R/FR
Low R/FR
Col
hfr1
pif4pif5
hfr1pif4pif5
B
PIL1
Relative expression
500
400
300
200
100
0
High R/FR
Low R/FR
Col
hfr1
pif4pif5
hfr1pif4pif5
XTR7
Relative expression
120
100
80
60
40
20
0
High R/FR
Low R/FR
Col
hfr1
pif4pif5
hfr1pif4pif5

Figure 2

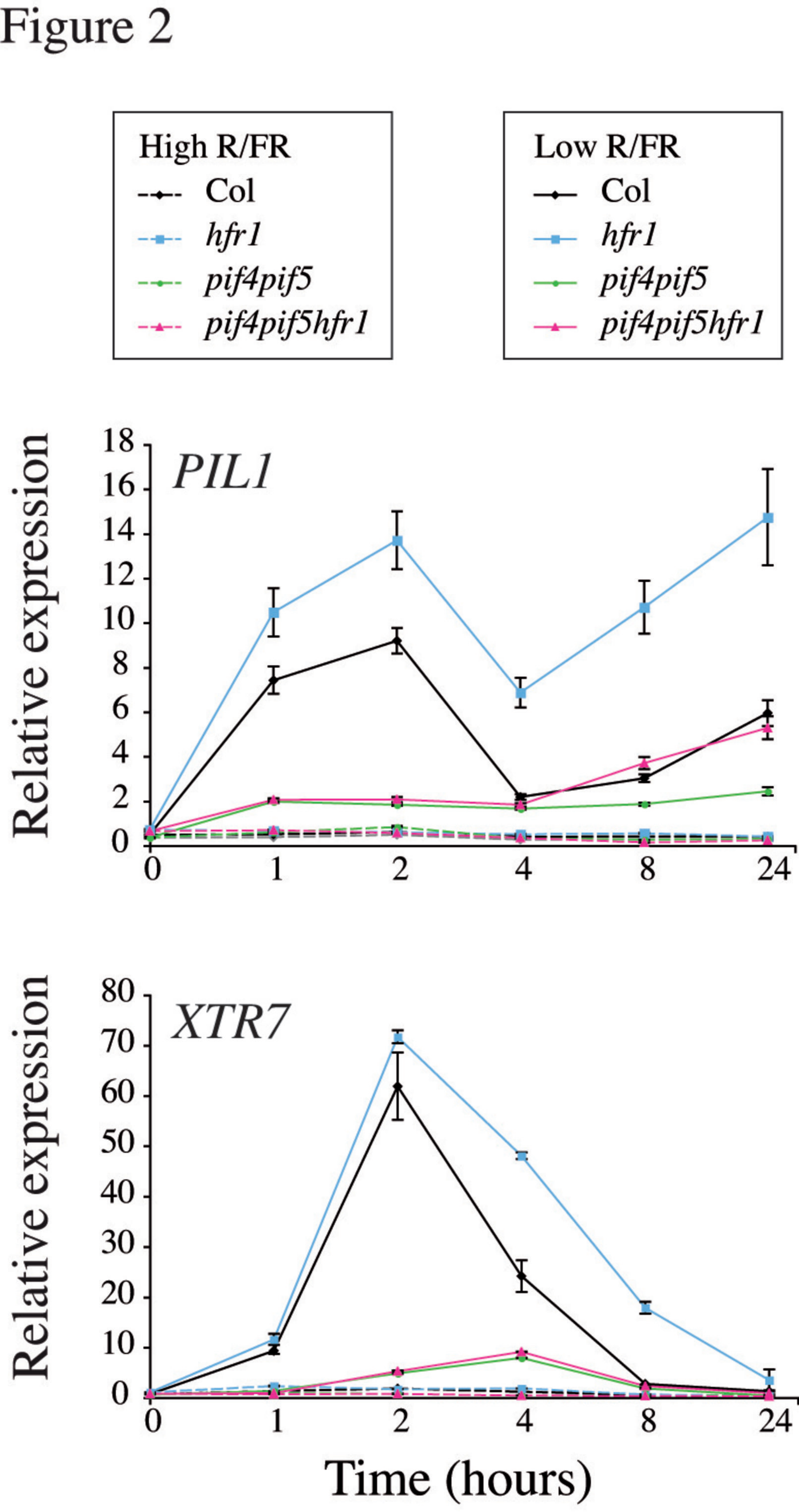
High R/FR
Col
hfr1
pif4pif5
pif4pif5hfr1
Low R/FR
Col
hfr1
pif4pif5
pif4pif5hfr1
PIL1
XTR7
Relative expression
Time (hours)
0
1
2
4
8
24

Figure 3

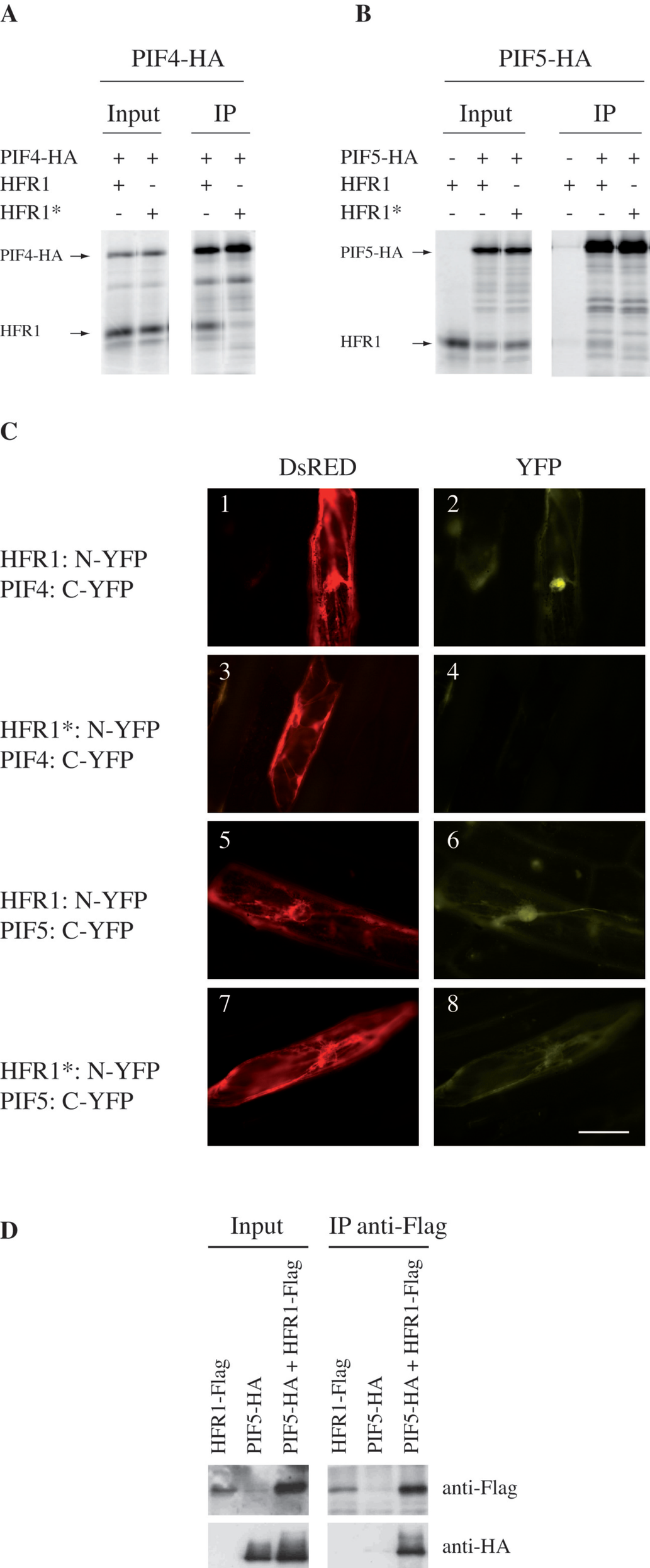
A
PIF4-HA
Input
IP
PIF4-HA + + + +
HFR1 + - + -
HFR1* - + - +
PIF4-HA
HFR1
B
PIF5-HA
Input
IP
PIF5-HA - + + - + +
HFR1 + + - + + -
HFR1* - - + - - +
PIF5-HA
HFR1
C
DsRED
YFP
HFR1: N-YFP
PIF4: C-YFP
HFR1*: N-YFP
PIF4: C-YFP
HFR1: N-YFP
PIF5: C-YFP
HFR1*: N-YFP
PIF5: C-YFP
1
2
3
4
5
6
7
8
D
Input
IP anti-Flag
HFR1-Flag
PIF5-HA
PIF5-HA + HFR1-Flag
HFR1-Flag
PIF5-HA
PIF5-HA + HFR1-Flag
anti-Flag
anti-HA

Figure 4

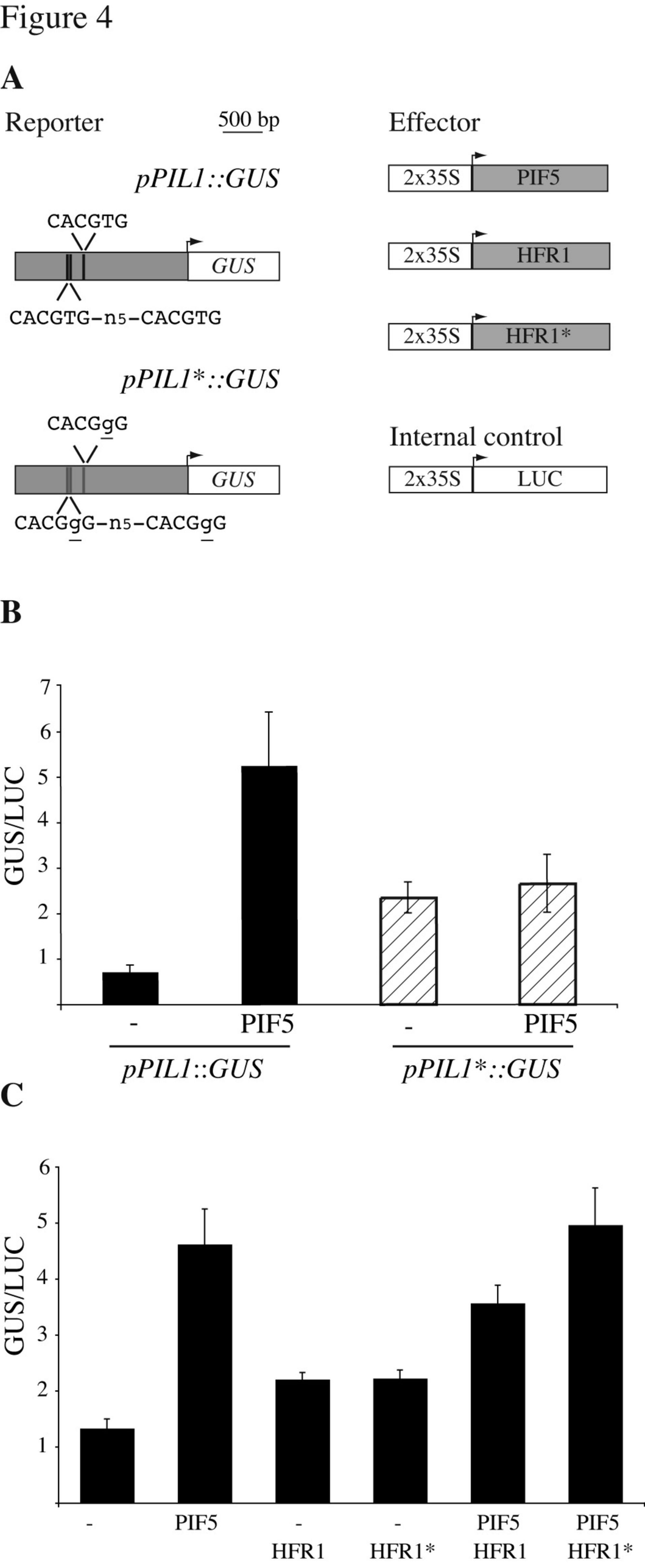
A
Reporter
500 bp
Effector
pPIL1::GUS
CACGTG
GUS
CACGTG-n5-CACGTG
2x35S
PIF5
2x35S
HFR1
2x35S
HFR1*
pPIL1*::GUS
CACGgG
GUS
CACGgG-n5-CACGgG
Internal control
2x35S
LUC
B
GUS/LUC
7
6
5
4
3
2
1
-
PIF5
-
PIF5
pPIL1::GUS
pPIL1*::GUS
C
GUS/LUC
6
5
4
3
2
1
-
PIF5
-
HFR1
-
HFR1*
PIF5
HFR1
PIF5
HFR1*

Figure 5

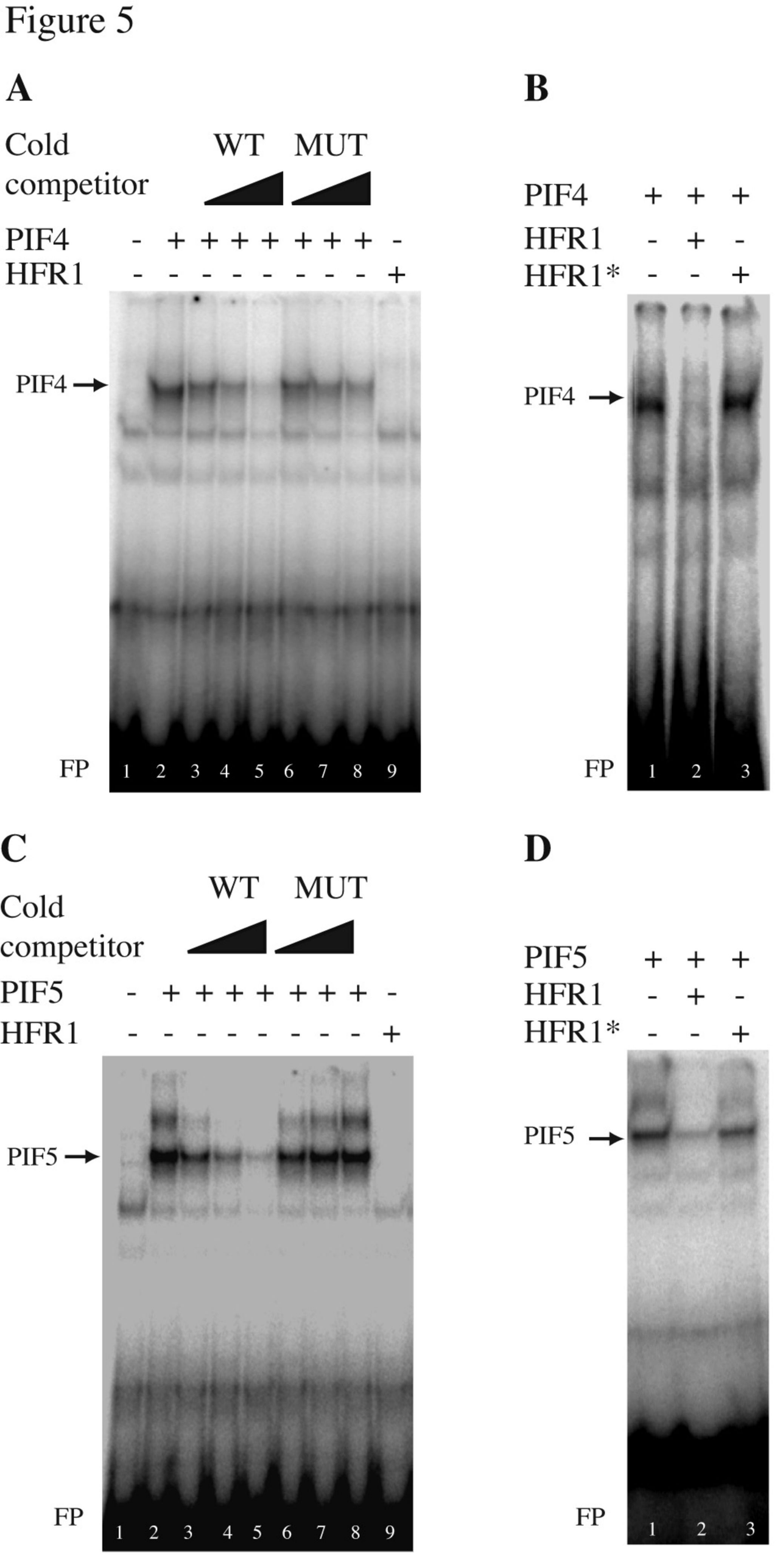
A
Cold competitor
WT
MUT
PIF4 - + + + + + + + -
HFR1 - - - - - - - - +
PIF4
FP
1 2 3 4 5 6 7 8 9
B
PIF4 + + +
HFR1 - + -
HFR1* - - +
PIF4
FP
1 2 3
C
Cold competitor
WT
MUT
PIF5 - + + + + + + + -
HFR1 - - - - - - - - +
PIF5
FP
1 2 3 4 5 6 7 8 9
D
PIF5 + + +
HFR1 - + -
HFR1* - - +
PIF5
FP
1 2 3

Figure 6

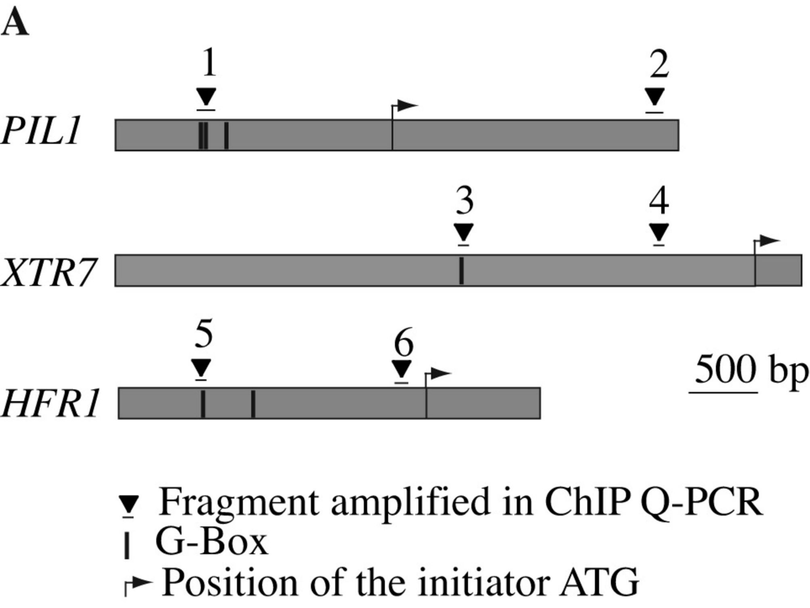
A
1
2
PIL1
3
4
XTR7
5
6
HFR1
500 bp
Fragment amplified in ChIP Q-PCR
G-Box
Position of the initiator ATG

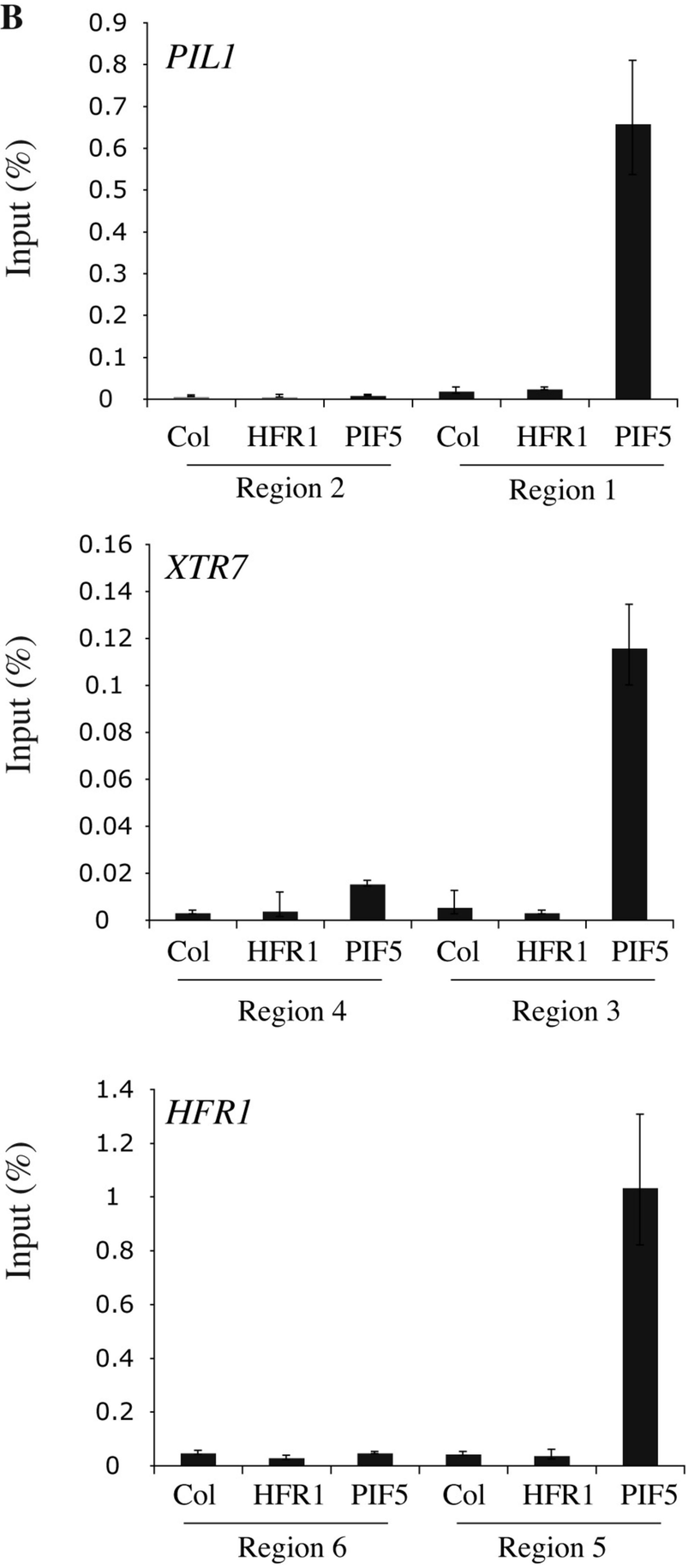
B
PIL1
Input (%)
0.9
0.8
0.7
0.6
0.5
0.4
0.3
0.2
0.1
0
Col HFR1 PIF5 Col HFR1 PIF5
Region 2
Region 1
XTR7
Input (%)
0.16
0.14
0.12
0.1
0.08
0.06
0.04
0.02
0
Col HFR1 PIF5 Col HFR1 PIF5
Region 4
Region 3
HFR1
Input (%)
1.4
1.2
1
0.8
0.6
0.4
0.2
0
Col HFR1 PIF5 Col HFR1 PIF5
Region 6
Region 5

Inhibition of the shade avoidance response by formation of non-DNA binding bHLH heterodimers.

Patricia Hornitschek, Séverine Lorrain, Vincent Zoete, Olivier Michielin and Christian Fankhauser

Supplemental Information.

Supplemental Materials and methods

Generation of transgenic plants

To generate plants expressing HA-tagged versions of HFR1 or HFR1* (mutated version of HFR1 in the HLH domain) HFR1-3xHA was generated by PCR using the primers pSP5 and pSP27. The PCR product was digested with KpnI and XhoI and ligated into the binary plant vector pCHF6 digested with KpnI and SalI. HFR1* was generated by site directed mutagenesis using the primers pPH20 and pPH21 using the QuikChange Site-Directed Mutagenesis Kit from Stratagene. The contructs carrying HFR1 (PH49) or HFR1* (PH51) fused to a triple HA under the control of the cauliflower mosaic virus promoter 35S were transformed into *hfr1* plants. Transformants with a 3:1 segregation ratio were self-fertilized, and homogenous progeny were selected. Primer sequences are given on table I.

Homology modeling

The PIF4 (UniProt (Boeckmann et al., 2003) entry Q8W2F3, residues 258 to 314), PIF5 (Uniprot entry Q84LH8, residues 257 to 313) and HFR1 (UniProt entry Q9FE22, residues 135 to 191) sequences were defined as target sequences for homology modeling. Experimental crystal structures of the human SREBP-1A (PDB (Parraga et al., 1998) ID 1AM9 (Parraga et al., 1998), and the mouse and human Max transcription factors (PDB ID 1AN2 (Ferre-D'Amare et al., 1993) and 1HLO (Brownlie et al., 1997), respectively) were used as structural templates. In these reference structures, the basic Helix-Loop-Helix transcription factors bind as dimers to their recognition DNA sequence by direct contacts between the alpha-helical basic region and the major groove of the DNA helix. This allows building structural models

of the PIFs and HFR1 homodimers and heterodimers bound to the DNA CACGTG E-box. It is interesting to note that the recognition sequence of Max is identical to that of the PIFs, i.e. CACGTG, so that relevant interactions between the PIF homodimers and the G-box can be expected in the homology model.

The multiple sequence alignment of the target and template sequences was realized using the MUSCLE algorithm (Edgar, 2004). Based on that target-template sequence alignment, model structures of HFR1/HFR1, PIFs/PIFs and HFR1/PIF4 or HFR1/PIF5 dimers bound to the DNA GCGGCATT*CACGTG*AAGTGCAC sequence of the *PIL1* promoter, which includes the CACGTG G-box were build by satisfaction of spatial restraints using the MODELLER program (Sali and Blundell, 1993). 500 models were built for each complex. The final model, selected based on the modeller objective function, was energy minimized using the CHARMM program and the CHARMM27 all atom force field (MacKerell et al., 2000) to remove the limited sterical clashes arising from the model building. The minimization consisted of 100 steps of steepest descent using a dielectric constant of 1 and a harmonic 5 $kcal.mol^{-1}Å^{-2}$ restrain on the backbone atoms.

Supplementary Table I:

List of primers used in this study

pPH9: ACGGGATCCTGAAGTAAACTGAACAAAGC

pPH17: TGCGAATTCCGTATTCGTATAGAATAGTT

pPH20: CAAGACGGACAAGGTTTCGGATGAGGACAAGACCATAGAG

pPH21: CTCTATGGTCTTGTCCTCATCCGAAACCTTGTCCGTCTTG

pPH24: ATGGGAGCTCTAGTCTTCTCATCGCA

pPH45: CGCGGCATTCACGGGAAGTGCACGGGAACTTGGCC

pPH46: GGCCAAGTTCCCGTGCACTTCCCGTGAATGCCGCG

pPH47: GGTTCTTTCCGCTCACGGGGGCCTTTTGTGCC

pPH48: GGC ACA AAA GGC CCC CGT GAG CGG AAA GAA CC

pPH49: GGAAGCAAAACCCTTAGCATCAT

pPH50: TCCATATAATCTTCATCTTTTAATTTTGGTTTA

pPH78: GAATCACGCGGCATTCAC

pPH79: ACCTTCACGCCATTATTAAGAC

pPH112: ACGTGATGCCCTCGTGATGGAC

pPH113: GTCGCTCGCTAAGACACCAAC

pPH120: CGCATGCCGGCTGGAATAGATAG

pPH121: CGACGTGTCACTTCCCTCGTACC

pPH126: ACGCAACAAACGAACCACAC

pPH127: AGAGCGATCGGATCAGATAG

pPH130: TCGAGGTATGATGGGTGTAG

pPH131: GCTGAGAACACTGAGTACTG

pPL8F: GGGATGAACAATGCACCACCACAA

pPL8R: AAACACACGAAGGCACCACGAATG

Mt121: CGGCTTGCACAGCCTCTT

Mt122: TCGGTTGCCACTTGCAATT

Mt123: CATCGGTGTGGCCTTGAAA

MT124: CCAGTCTCCATCTTTGTCTTCGTA

Mt157: CTTCCAAGGGAAAGAGGGTGA

Mt158: TTCCGCAAAGATCTTCCATGTAAC

SL44: GATGCGTAAGCTACAGCAACTCGT

SL45: AGAACCGAAACCTTGTCCGTCTTG

pSP05: TAGAATTCGGTACCAACATGTCGAATAATCAAGCTTTC

pSP27: GAACGTCATATGGATAGGATCCTGCATAGTCCGGGA

F_*EF1α*: TGGTGTCAAGCAGATGATTTGC

R_ *EF1α*: ATGAAGACACCTCCTTGATGATTTC

F_*GAPC-2*: GCAAAATGGCTGACAAGAAGATC

R_*GAPC-2* AGCAACCAAACGACCGATTC

FGbox: acgcggcattcacgtgaagtgcacgtgaacttggcca

RGbox: tggccaagttcacgtgcacttcacgtgaatgccgcgt

FGbox-Mt: acgcggcattcacgGgaagtgcacgGgaacttggcca

RGbox-Mt: tggccaagttcCcgtgcacttcCcgtgaatgccgcgt

Supplemental Figure legends

Supplemental Figure S1

PIF4 and PIF5 are necessary for a full induction of *HFR1* in response to shade.

Wild-type and *pif4pif5* seedlings were grown for 8.5 days in high R/FR (white bars) or for 4 days in high R/FR subsequently for 4.5 days in low R/FR (black bars).

HFR1 expression was analyzed by Q-PCR analysis. Expression is shown relative to Col-0 in high R/FR. Three biological replicas were performed with three technical replicates for each sample. Values were normalized with *EF1α* and *GAPC-2*. Error bars represent SE.

Supplemental Figure S2. PIF4 and PIF5 do not play an important role in the expression of *IAA19* and *IAA29* in early-responses to shade.

Seedlings were grown for 6 days in high R/FR (12 h light / 12h dark) and then either kept in high R/FR ratios or shifted to low R/FR ratios.

The expression of *IAA19* and *IAA29* was analyzed by Q-PCR. Relative expressions to Col-0 (point 0) are shown for the different genotypes. Three biological replicas were performed with three technical replicates for each. Values were normalized with *EF1α* and *GAPC-2*. Error bars represent SE; n=100.

Supplemental Figure S3.

The *pif4pif5* mutations are epistatic over *hfr1* in early-responses to shade.

Seedlings were grown for 6 days in high R/FR (constant light) and then either kept in high R/FR ratios or shifted to low R/FR ratios.

The expression of *PIL1* and *XTR7* was analyzed by Q-PCR. Relative expressions to Col-0 (point 0) are shown for the different genotypes. Three technical replicas were performed for each sample. Values were normalized with *EF1α* and *GAPC-2*. Error bars represent SE.

Supplemental Figure S4. HFR1 dimerization is required for its activity

(A) Schematic presentation of the HLH domain of HFR1 indicating the mutated residues of HFR1*. (**B**) Hypocotyl elongation was measured of 8.5-day-old seedlings, which were grown in high R/FR (white bars) or for 4 days in high R/FR subsequently for 4.5 days in low R/FR (black bars). Data are the means ± SD; n=15. (**C**) Accumulation of the HFR1-HA or HFR1*-HA proteins in response to shade. 4-day-

old etiolated seedlings were transferred for 3 h to shade and total proteins were extracted. Protein accumulation was analyzed by western blotting using the anti-HA antibody. Membrane stained with Ponceau S is shown as a loading control.

Supplemental Figure S5. Homology modeling predicts that HFR1 prevents PIF4 and PIF5 from DNA binding to the *PIL1* promoter sequence

(**A**) Homology modeling of the PIF5 homodimer to the *PIL1* promoter sequence. (**B**) Homology modeling of the HFR1/PIF5 heterodimer to the *PIL1* promoter sequence.

Supplemental Figure S6:

In vitro transcribed and translated, ^{35}S Met labeled proteins used for the experiment presented on Figure 6 were resolved by SDS-PAGE and visualized by autoradiography. (**A**) PIF4/HFR1 (**B**) PIF5/HFR1

Supplementary References

Boeckmann, B., Bairoch, A., Apweiler, R., Blatter, M.C., Estreicher, A., Gasteiger, E., Martin, M.J., Michoud, K., O'Donovan, C., Phan, I., Pilbout, S. and Schneider, M. (2003) The SWISS-PROT protein knowledgebase and its supplement TrEMBL in 2003. *Nucleic Acids Res*, **31**, 365-370.

Brownlie, P., Ceska, T., Lamers, M., Romier, C., Stier, G., Teo, H. and Suck, D. (1997) The crystal structure of an intact human Max-DNA complex: new insights into mechanisms of transcriptional control. *Structure*, **5**, 509-520.

Edgar, R.C. (2004) MUSCLE: multiple sequence alignment with high accuracy and high throughput. *Nucleic Acids Res*, **32**, 1792-1797.

Ferre-D'Amare, A.R., Prendergast, G.C., Ziff, E.B. and Burley, S.K. (1993) Recognition by Max of its cognate DNA through a dimeric b/HLH/Z domain. *Nature*, **363**, 38-45.

MacKerell, A.D., Jr., Banavali, N. and Foloppe, N. (2000) Development and current status of the CHARMM force field for nucleic acids. *Biopolymers*, **56**, 257-265.

Parraga, A., Bellsolell, L., Ferre-D'Amare, A.R. and Burley, S.K. (1998) Co-crystal structure of sterol regulatory element binding protein 1a at 2.3 A resolution. *Structure*, **6**, 661-672.

Sali, A. and Blundell, T.L. (1993) Comparative protein modelling by satisfaction of spatial restraints. *J Mol Biol*, **234**, 779-815.

S_Figure 1

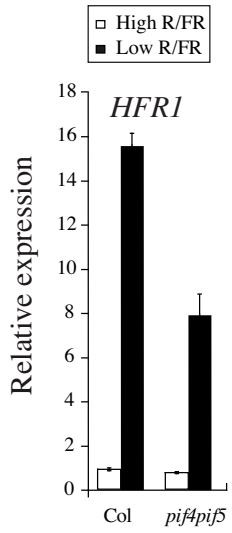
High R/FR
Low R/FR
HFR1
Relative expression
18
16
14
12
10
8
6
4
2
0
Col
pif4pif5

S_Figure 2

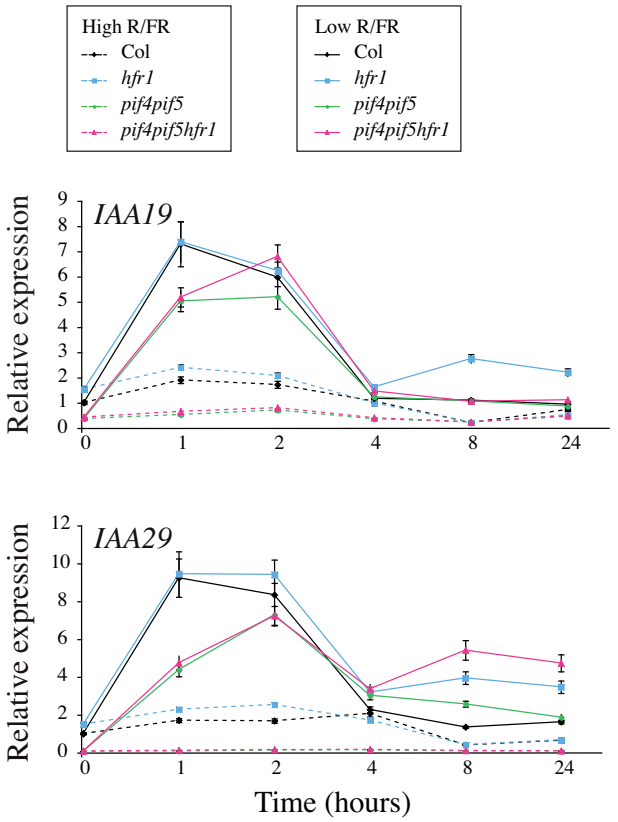
High R/FR
Col
hfr1
pif4pif5
pif4pif5hfr1
Low R/FR
Col
hfr1
pif4pif5
pif4pif5hfr1
IAA19
Relative expression
0
1
2
3
4
5
6
7
8
9
0
1
2
4
8
24
IAA29
Relative expression
0
2
4
6
8
10
12
0
1
2
4
8
24
Time (hours)

S_Figure 3

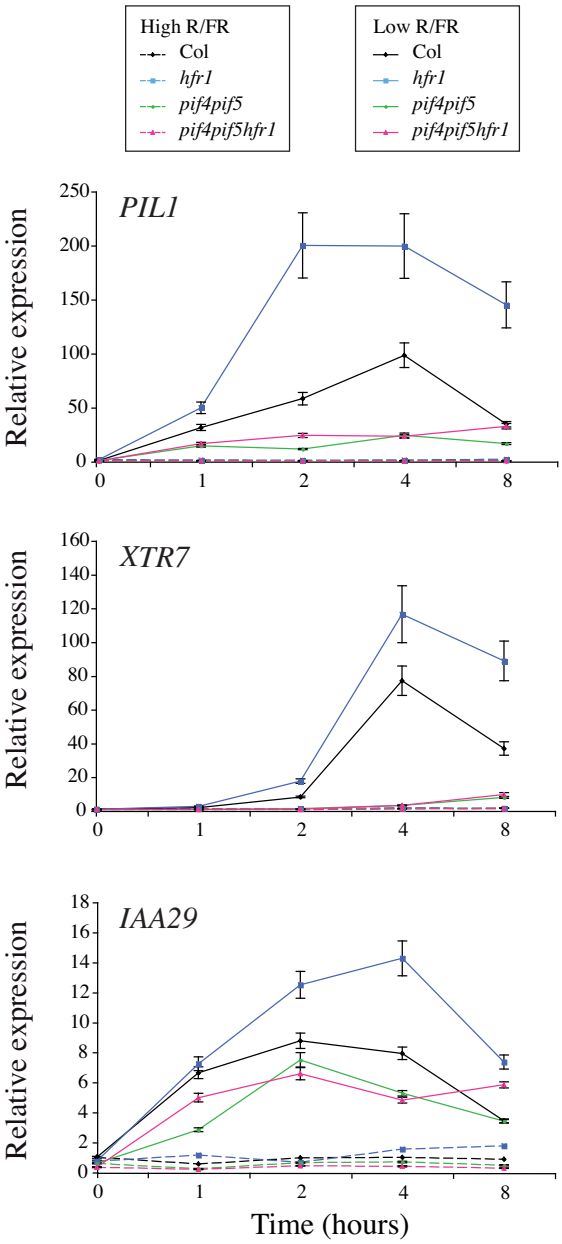
High R/FR
Col
hfr1
pif4pif5
pif4pif5hfr1
Low R/FR
Col
hfr1
pif4pif5
pif4pif5hfr1
PIL1
XTR7
IAA29
Relative expression
Relative expression
Relative expression
Time (hours)

S_Figure 4

A

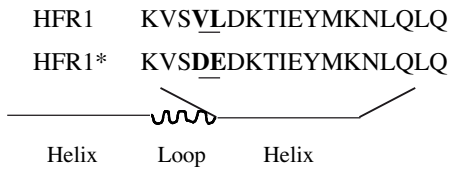

B

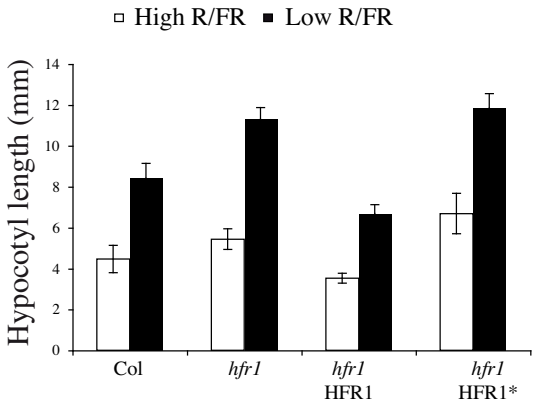

C

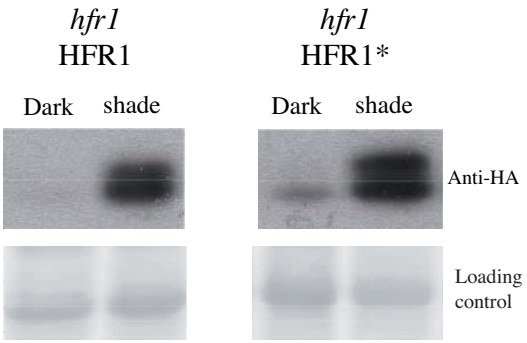

S_Figure 5

A

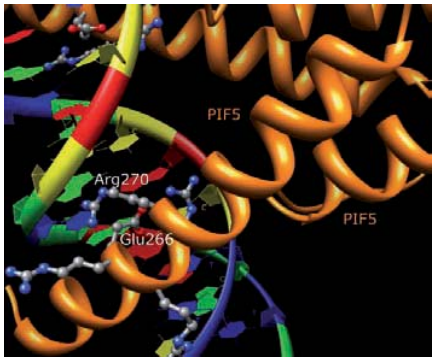

B

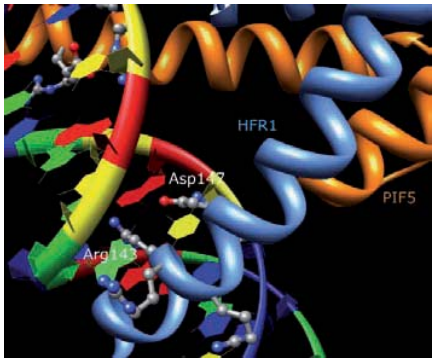

S_Figure 6